

# Establishing the Relationship Between GMI and SNR in Optical Networks with Nonlinear Kerr Effect

Xueying Zhong<sup>(1)</sup>, Huazhi Lun<sup>(1)</sup>, Mengfan Fu<sup>(1)</sup>, Xiaomin Liu<sup>(1)</sup>, Lilin Yi<sup>(1)</sup>, Weisheng Hu<sup>(1)</sup>,  
Qunbi Zhuge<sup>(1)</sup>

<sup>(1)</sup> State Key Laboratory of Advanced Optical Communication Systems and Networks, Department of Electronic Engineering, Shanghai Jiao Tong University, Shanghai 200240, China, [qunbi.zhuge@sjtu.edu.cn](mailto:qunbi.zhuge@sjtu.edu.cn)

**Abstract** We propose an artificial neural network (ANN) based algorithm to establish the mapping between generalized mutual information (GMI) and signal-to-noise ratio (SNR) in optical networks with nonlinear Kerr effect. Under highly diverse link configurations, the network achieves great performance with 0.043 dB maximum absolute error.

## Introduction

With the rapid development of high-definition video streaming, cloud computing, 5G, and so on, the requirement for the capacity of optical communication system is growing exponentially. In this context, leveraging the unnecessary margins is a path to increase the capacity [1]. To achieve that, a proper metric for evaluating margin is essential. Although metrics based on the pre-forward-error-correction (pre-FEC) bit error rate (BER) such as the signal-to-noise ratio (SNR) are widely used [2-3], they may be improper for current systems that adopt soft-decision FEC. Consequently, finding a better metric is essential, and the generalized mutual information (GMI) can be a proper candidate [4]. However, compared with SNR, the physical meaning of GMI is not intuitive. To acquire SNR margin from GMI margin, the SNR threshold value should be calculated with the GMI threshold value. Therefore, building the mapping relationship between SNR and GMI is essential. Although the corresponding relationship is explicit in an additive white Gaussian noise (AWGN) channel, the study of the influence of fibre nonlinear Kerr effect is still limited.

In this paper, we propose an artificial neural network (ANN) based algorithm to establish the mapping between SNR and GMI considering a nonlinear fibre channel. The adopted features are extracted from the coherent receiver. Since no additional devices are needed, it can achieve a low-cost implementation. To verify the proposed algorithm, extensive simulations are performed. The maximum absolute error is only 0.043 dB, demonstrating a high accuracy of the proposed method.

## Principle

Fig. 1(a) depicts the block diagram of the proposed algorithm. In the digital signal processing module, features are firstly extracted

from the carrier phase recovery (CPR) module and then sent to the pre-processing module, whose outputs will be as inputs of the ANN. After training, ANN can establish a proper mapping between GMI and SNR.

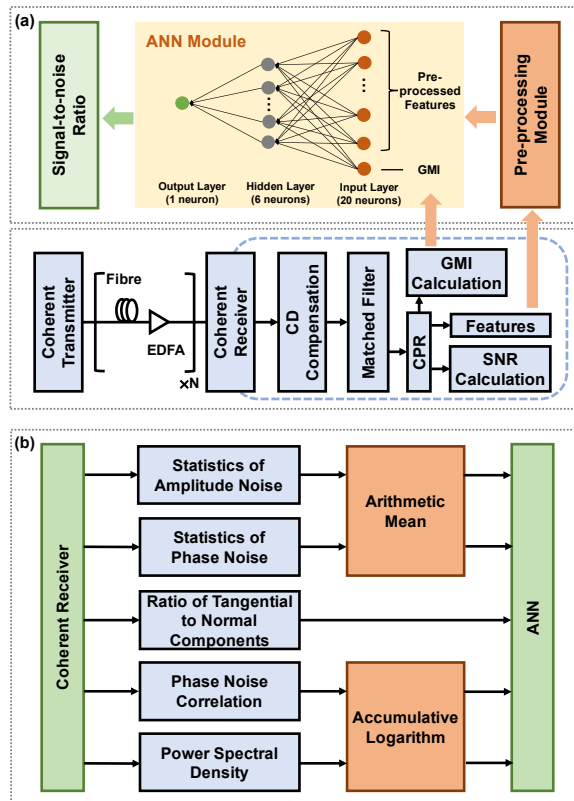


**Fig. 1:** (a) The block diagram of the proposed algorithm. (b) Features and the pre-processing module.

Features and the pre-processing module are shown in Fig. 1(b). For pre-processing, the amplitude noise (AN) and phase noise (PN) are first calculated. Since the nonlinear interference (NLI) noise caused by the nonlinear Kerr effect is a kind of colored noise, the statistic value of AN and PN can be quite different from the AWGN. Consequently, we first calculate statistics described in [5]. In Tab. 1, the adopted statistics

Tab. 1: Description of used statistics.

Statistic	Formula
Mean ( $\mu$ )	$\mu = E\{x\}$
Standard deviation ( $\sigma$ )	$\sigma = \sqrt{E\{(x - \mu)^2\}}$
Median ( $m$ )	$\int_{-\infty}^m pdf_X(x) dx = 0.5$
Mode ( $m_o$ )	The most frequent value
Skew	$E\left\{\left(\frac{x - \mu}{\sigma}\right)^3\right\}$
Pearson's first coefficient	$(\mu - m)/\sigma$
Asymmetry measure	$1^{st}P + 99^{st}P - 2 \times m_o$

are summarized, where  $x$  represents the AN / PN,  $E$  represents the expectation,  $pdf_X$  represents the probability density function, and  $P$  represents percentile.

After that, we analyse the constellation diagram. For each individual symbol, tangential and normal components are calculated. For each ring, average values of those two components are employed to alleviate the influence of random fluctuations. As is shown in Fig. 2, ratios between tangential and normal components are calculated.

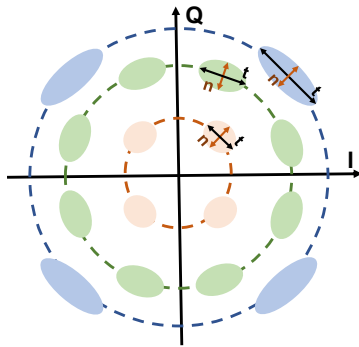


Fig. 2: Tangential and normal components.

Since the ratios calculated above represent the correlation of the PN caused by the nonlinear Kerr effect [6], we further calculate the accumulative logarithmic of PN correlation according to Eq. (1) – Eq. (2):

$$PNC = \text{corr}(\Delta\theta_k, \Delta\theta_{k+m}), \quad (1)$$

$$ALPNC = 10 \log_{10} \left\{ 1 / \sum_{i=1}^n |PNC_i| \right\} \quad (2)$$

where  $\Delta\theta_k$  refers to the phase noise of the  $k_{th}$  received symbol, and  $n$  refers to the correlation length. For ALPNC, we set  $n$  to 60.

Finally, the power spectral density of the phase noise is calculated. All those features above are as inputs of the ANN, and after training, the relationship between GMI and SNR can be established.

## Simulation Setup

The simulation setup is shown in Fig. 3. The modulation format is 16 quadrature amplitude modulation (QAM) with a symbol rate of 35 GBaud. The number of wavelength division multiplexing (WDM) channels ranges from 7 to 21 with a step size of 2. A root-raised-cosine (RRC) filter with a roll-off rate of 0.02 is applied for pulse shaping. After that, the signal is launched into the link with a launch power swept from -1 dBm to 3 dBm.

For the link, the type of each span is randomly chosen between the standard single mode fibre (SSMF) and the enhanced large effective area fibre (ELEAF). The length of each span is set to 80 km, and the span number is swept from 8 to 15. At the end of each span, an erbium-doped fibre amplifier (EDFA) with a noise figure of 5 dB is used to compensate the fibre loss. The nonlinear Kerr effect is simulated using the split-step Fourier method (SSFM) with a step size of 20 m.

At the receiver side, the centre channel is filtered out. The chromatic dispersion (CD) compensation is first applied, followed by the matched filter and the CPR. Finally, we generate 960 samples for training ANN. 85% of them are for training, and the rest samples are for testing.

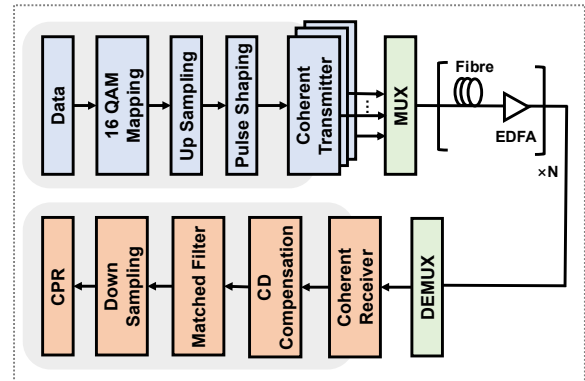


Fig. 3: Simulation setup.

## Results and Discussions

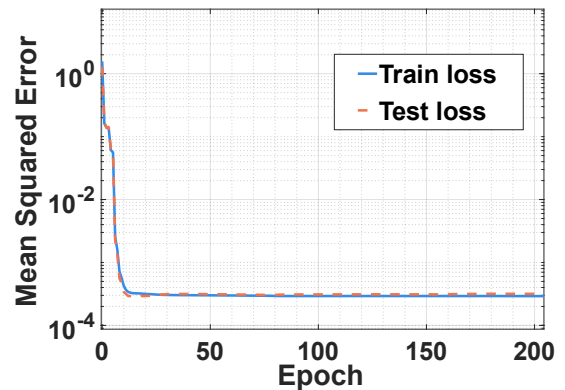


Fig. 4: The loss curves of training and testing.

Fig. 4 plots the learning curve of the proposed algorithm. It can be observed that the two curves are close and the algorithm has converged, meaning that no overfitting occurs.

To evaluate the performance of ANN, we analyse all 144 data samples in the testing dataset. Results are shown in Fig. 5. In Fig. 5(a), The blue dots represent the results obtained using the relationship between SNR and GMI in the AWGN channel. It can be seen that a large error exists, meaning that the relationship is not proper for the scenario when nonlinear Kerr effect cannot be neglected. Compared with results above, our method can have a much more accurate result with the maximum absolute error less than 0.05 dB, which demonstrates the superior performance of the proposed method.

In Fig. 5(b), the error histograms are shown. The error without ANN ranges from -0.500 dB to -0.004 dB, while the error of the proposed method ranges from -0.040 dB to 0.043 dB, indicating a significant performance improvement.

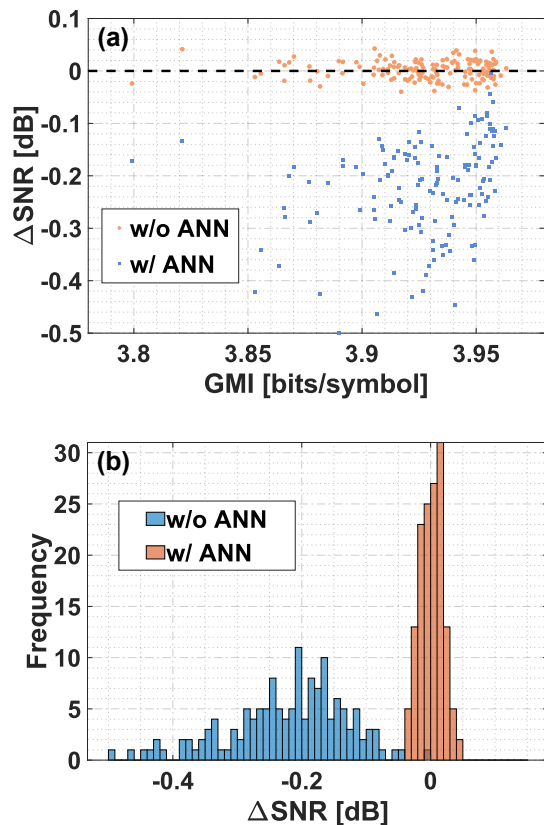


Fig. 5: (a) The scatter plots of the estimated errors with and without ANN. (b) The error histograms of SNR estimation.

In Fig. 6, the cumulative histograms of the absolute error are shown. When the absolute error is 0.05 dB, the cumulative values are 3 and 144, respectively. Results reveal that the SNR error values are smaller and the distribution is more concentrated with our method.

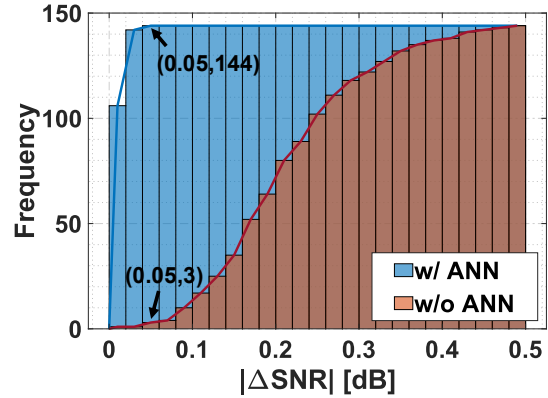


Fig. 6: The cumulative histograms of the absolute error.

## Conclusion

In this paper, we propose an ANN based algorithm to establish the mapping between SNR and GMI for the scenario when nonlinear Kerr effect cannot be neglected. Features we used are extracted from the coherent receiver. Under highly diverse link configurations, the network achieves great performance with 0.043 dB maximum absolute error.

## Acknowledgements

This work was supported by National Key R&D Program of China (2018YFB1800902), and National Natural Science Foundation of China (62175145).

## References

- [1] Y. Pointurier, "Design of low-margin optical networks," 2016 Optical Fiber Communications Conference and Exhibition (OFC), 2016, pp. 1-3. DOI: [10.1364/JOCN.9.0000A9](https://doi.org/10.1364/JOCN.9.0000A9)
- [2] F. Golaghazadeh, P. Djukic, C. Tremblay, and C. Desrosiers, "Forecasting SNR margins has low-complexity," in OSA Advanced Photonics Congress (AP) 2020 (IPR, N P, NOMA, Networks, PVLED, PSC, SPPCom, SOF), L. Caspani, A. Tauke-Pedretti, F. Leo, and B. Yang, eds., OSA Technical Digest (Optica Publishing Group, 2020), paper NeW1B.4. DOI: [10.1364/NETWORKS.2020.NeW1B.4](https://doi.org/10.1364/NETWORKS.2020.NeW1B.4)
- [3] E. Seve, J. Pesic, C. Delezoide, S. Bigo and Y. Pointurier, "Learning process for reducing uncertainties on network parameters and design margins," in Journal of Optical Communications and Networking, vol. 10, no. 2, pp. A298-A306, Feb. 2018. DOI: [10.1364/JOCN.10.00A298](https://doi.org/10.1364/JOCN.10.00A298)
- [4] A. Alvarado, E. Agrell, D. Lavery, R. Maher and P. Bayvel, "Replacing the Soft-Decision FEC Limit Paradigm in the Design of Optical Communication Systems," in Journal of Lightwave Technology, vol. 33, no. 20, pp. 4338-4352, 15 Oct. 15, 2015. DOI: [10.1109/JLT.2015.2450537](https://doi.org/10.1109/JLT.2015.2450537)
- [5] A. Salehiomran, G. Gao and Z. Jiang, "Linear and nonlinear noise monitoring in coherent systems using fast BER measurement and neural networks," 45th European Conference on Optical Communication (ECOC 2019), 2019, pp. 1-3. DOI: [10.1049/cp.2019.0956](https://doi.org/10.1049/cp.2019.0956)
- [6] F. J. V. Caballero et al., "Machine learning based linear and nonlinear noise estimation," in Journal of Optical Communications and Networking, vol. 10, no. 10, pp. D42-D51, Oct. 2018. DOI: [10.1364/JOCN.10.000D42](https://doi.org/10.1364/JOCN.10.000D42)